# Global Perspective of the Quasi-Biweekly Oscillation*

KAZUYOSHI KIKUCHI AND BIN WANG

*International Pacific Research Center, University of Hawaii at Manoa, Honolulu, Hawaii*

(Manuscript received 6 December 2007, in final form 10 September 2008)

ABSTRACT

The quasi-biweekly oscillation (QBW: here defined as a 12–20-day oscillation) is one of the major systems that affect tropical and subtropical weather and seasonal mean climate. However, knowledge is limited concerning its temporal and spatial structures and dynamics, particularly in a global perspective. To advance understanding of the QBW, its life cycle is documented using a tracking method and extended EOF analysis. Both methods yield consistent results. The analyses reveal a wide variety of QBW activity in terms of initiation, movement, development, and dissipation. The convective anomalies associated with the QBW are predominant in the latitude bands between 10° and 30° in both hemispheres. The QBW modes tend to occur regionally and be associated with monsoons. Three boreal summer modes are identified in the Asia–Pacific, Central America, and subtropical South Pacific regions. Five austral summer modes are identified in the Australia–southwest Pacific, South Africa–Indian Ocean, South America–Atlantic, subtropical North Pacific, and North Atlantic–North Africa regions.

The QBW modes are classified into two categories: westward- and eastward-propagating modes. The westward mode is found in the Asia–Pacific and Central America regions during boreal summer; it originates in the tropics and dissipates in the subtropics. The behavior of the westward-propagating mode can be understood in terms of equatorial Rossby waves in the presence of monsoon mean flow and convective coupling. The eastward-propagating mode, on the other hand, connects with upstream extratropical Rossby wave trains and propagates primarily eastward and equatorward. Barotropic Rossby wave trains play an essential role in controlling initiation, development, and propagation of the eastward QBW mode in the subtropics. The results therefore suggest that not only tropical but also extratropical dynamics are required for fully understanding the behavior of the QBW systems worldwide. The new conceptual picture of QBW obtained here based on long-term observation provides valuable information on the behavior of QBW systems in a global perspective, which is important for a thorough understanding of tropical variability on a time scale between day-to-day weather and the Madden–Julian oscillation.

## 1. Introduction

Quasi-biweekly (QBW) variation is one of the most important components of the tropical variation on a time scale in between day-to-day weather and the Madden–Julian oscillation (MJO) (Madden and Julian 1971, 1972). In the Indian Ocean and western Pacific, predominant 10–20-day periodicity has been found in precipitation and horizontal winds through spectral analyses (Murakami and Frydrych 1974; Murakami 1975; Zangvil 1975; Krishnamurti and Bhalme 1976; Krishnamurti and Ardanuy 1980; Chen and Chen 1993; Kiladis and Wheeler 1995; Numaguti 1995). The QBW, by its periodicity, falls outside of the category of the MJO, which is characterized by a 40–50 or 30–60 day oscillation (Madden and Julian 1994). Sometimes, QBW variability is viewed as a high-frequency part of tropical intraseasonal variability (Zhang 2005; Waliser 2006).

Since the Asian summer monsoon is the most intensive among tropical monsoons, its behavior is of great scientific concern. Both the QBW and MJO influence the active/break cycles of Indian summer monsoon (Krishnamurti and Ardanuy 1980; Yasunari 1981; Goswami et al. 2003) and South China Sea monsoon (Chen et al. 2000; Chan et al. 2002; Mao and Chan 2005; Zhou and Miller 2005). Understanding of the two types of tropical intraseasonal oscillations (ISOs), the QBW

* School of Ocean and Earth Science and Technology Contribution Number 7558 and International Pacific Research Center Contribution Number 550.

*Corresponding author address:* Kazuyoshi Kikuchi, International Pacific Research Center, University of Hawaii at Manoa, 1680 East-West Road, Post Bldg. 401, Honolulu, HI 96822.
E-mail: kazuyosh@hawaii.edu

DOI: 10.1175/2008JCLI2368.1

and MJO, is imperative for comprehensively understanding of tropical variations on a time scale from daily to seasonal.

While its large impact on the Asian summer monsoon has been well recognized, the QBW on the global scale has not been discussed in the literature. As will be shown in sections 2 and 3, the QBW is a predominant component not only in the Asian summer monsoon region but also in other subtropical regions. Comprehensive understanding of the QBW is thus mandatory to develop our knowledge of tropical as well as subtropical meteorology. The purpose of this study is to document the QBW behavior in a global perspective based on long-term observational data. For this purpose, all possible QBW modes in various regions of the global tropics and subtropics will be detected and documented. The results obtained from this study suggest that there exist common mechanisms that control QBW behaviors even in different places and seasons.

This study will use two methods, namely a tracking method and an extended empirical orthogonal function (EEOF) analysis, to reveal its climatological life cycle, such as where it tends to occur, how it develops, and where it dissipates (see section 4 and 5). Theoretical interpretation of observational findings is given in section 6. A summary is presented in the last section.

## 2. Data and analysis methods

### *a. Data*

Outgoing longwave radiation (OLR) provides a reasonably good proxy for organized deep convection in the tropics. Long-term daily OLR data for the period 1979–2005 at 2.5° × 2.5 ° horizontal resolution (Liebmann and Smith 1996) were used in this study. To affirm the convective activity deduced from OLR data, the Tropical Rainfall Measuring Mission (TRMM) 3B42 version 6 precipitation dataset was also used. This dataset was provided with precipitation data, obtained by collecting passive microwave data and infrared data, in the entire tropics and beyond from 50°N to 50°S with high spatial (0.25° × 0.25°) and temporal (3 h) resolution since 1998 (Huffman et al. 2007). Daily data on coarser resolution of 2.5° × 2.5° was made and used in this study for the period 1998–2005. National Centers for Environmental Prediction–Department of Energy (NCEP–DOE) Atmospheric Model Intercomparison Project (AMIP)-II reanalysis winds in the troposphere from 1000 to 100 hPa at the horizontal resolution of 2.5° × 2.5° (Kanamitsu et al. 2002) were used to describe large-scale circulation associated with QBW for the period 1979–2005.

Before focusing on a specific time scale of the disturbance, we carried out a spectral analysis to identify the most significant periodicity of the variations because previous studies used different time filters, for example, 10–20 or 12–24 day by Chen and Chen (1993, 1995) and 6–30 day by Kiladis and Wheeler (1995). Eight locations for boreal summer and winter were selected in reference to the amplitude of intraseasonal variance whose periodicity is between about 6 and 60 days (Fig. 1).

### *b. Power spectral analysis*

The power spectral density (PSD) was computed using a standard approach (e.g., Emery and Thomson 1997) as follows. The seasonal cycle was removed by a Lanczos high-pass filter that significantly reduces the amplitude of the Gibbs oscillation (Duchon 1979) with a cutoff frequency of 121 days. Then the mean and linear trend were removed from the time series for a given season [e.g., extended boreal summer, May–September (MJJAS), and extended austral summer, November–March (NDJFM)] and a given year. After applying a 5% cosine taper to the time series to reduce end effects and sidelobe leakage, the PSD for a given season and year was obtained by means of a fast Fourier transform (FFT). The computed PSDs for a given season and year were the time mean PSD over 27 yr (27 extended summers and 26 extended winters) for a given location. Statistical significance was tested according to the method of Gilman et al. (1963) based on the power spectrum of red noise.

During northern summer (MJJAS), in most regions, the 30–60-day peak can be found (Fig. 2) except in the southern subtropics: the central South Pacific (Fig. 2e) and southeast coast of Brazil (Fig. 2h). This result seems reasonable because the effect of the MJO is expected to be small at these two locations far away from the equator. During southern summer (NDJFM), a significant 30–60-day peak can be found in all locations picked up here except Zimbabwe (Fig. 2i), Samoa (Fig. 2m), and the eastern North Pacific (Fig. 2n). Note that, since the core frequency of MJO can change with seasonal march and from year to year, the resultant mean spectrum is relatively smooth: thus, lack of a prominent peak in the mean spectrum does not necessarily mean that that part of the spectrum does not represent coherent variations.

What we would like to emphasize here is that spectral peaks can be found in the range of 12–20 days in some regions including the Arabian Sea, Bay of Bengal, South China Sea, subtropical central South Pacific, eastern North Pacific, and Caribbean Sea in MJJAS (Figs. 2a–c,e–g) and Zimbabwe, Australia, Samoa, the eastern North Pacific, and southeast of Brazil in NDJFM (Figs. 2i,k,m–o). Similarly, the peak associated with synoptic scale on the time scale of less than 10 days can be found in many regions in both seasons.

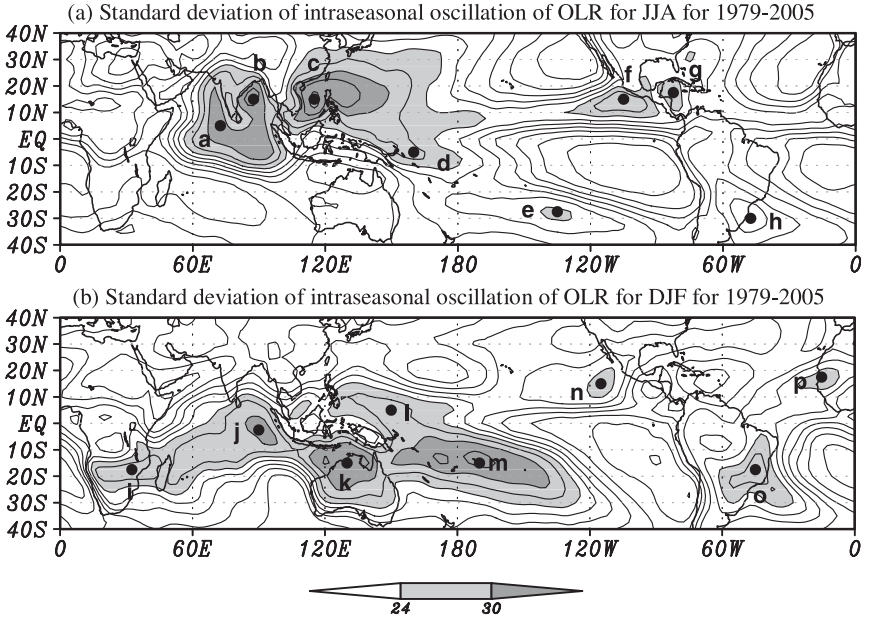


FIG. 1. Geographical distribution of the OLR standard deviation for intraseasonal oscillations (about 6–60 days) in (a) JJA and (b) DJF. The intraseasonal component was derived by applying a 60-day high-pass filter and then taking a 3-day running mean. Solid marks represent the places where the power spectrum is computed in Fig. 2.

### c. Temporal and spatial filtering

To extract disturbances associated with QBW, we apply two kinds of filters, namely temporal and spatial. Any field used in the tracking method and the EEOF analysis has been subjected to this filtering without exception.

First, we define the QBW time scale as 12–20 days in this study. A 10–20-day band could be another choice, but we would like to avoid those synoptic-scale disturbances whose periodicity is in the range of 8–11 days, which appear in selected places and are closer to synoptic disturbances (Lau and Lau 1990). Therefore the 12–20-day Lanczos bandpass filter was applied in this study. To describe the QBW disturbance we primarily examine OLR and zonal and meridional winds. This choice is consistent with the one previous work used for boreal summer (e.g., Chen and Chen 1993) and one for austral summer (e.g., Numaguti 1995), so this study can be easily compared with these previous studies and is a natural extension of the QBW study to the global scale. Also, note that the results in this study are not sensitive to whether we choose 12–20 days or 10–20 days or even broader 12–30 days for QBW filtering.

Next, an isotropic spatial filter developed by Sardeshmukh and Hoskins (1984) was employed to smooth out small-scale disturbances, which are probably not significant to QBW study. They introduced a spectral filter function

$$S_n = \exp\{n(n+1)/[n_0(n_0+1)]^r\}$$

to reduce the Gibbs phenomenon, where $n$ is the total wavenumber. With this filtering, the smoothed value $\bar{f}$ of $f$ at a given point $P_0$ can be expressed as

$$\bar{f} = \sum_{n=0}^{M} S_n \left(\frac{2n+1}{4\pi}\right)^{1/2} f'_n, \tag{1}$$

where $f'_n$ is the spectral coefficient in the rotated frame in which $P_0$ is the North Pole, and $M$ is truncation wavenumber. It is apparent that the properties of $S_n$ is completely determined by the total wavenumber $n$. In this study, total wavenumber 36 was adopted with parameters $n_0 = 18$ and $r = 1$. With this filtering, the weight function is reduced by half at about 5° away from a given grid so that the filtering does not considerably modulate the field (Sardeshmukh and Hoskins 1984).

### d. Tracking method

A tracking method is a useful technique to elucidate the essential features of a disturbance. Wang and Rui (1990) examined 122 ISO convective anomalies during 1979–89 using the same method and revealed many new features such as the origin, propagation, development, dissipation, and seasonality, which could not be revealed by spectral or other statistical analysis methods.

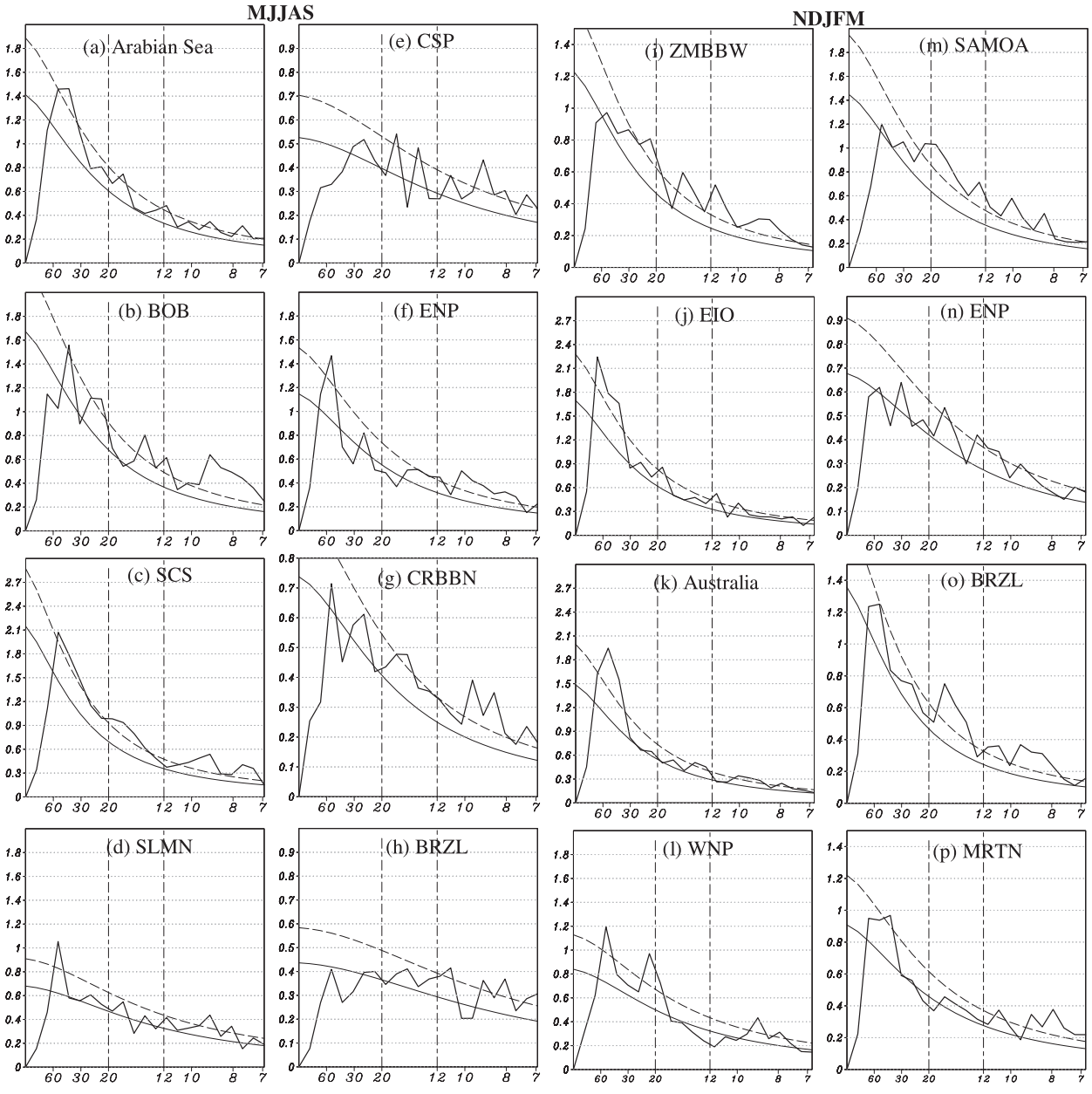


FIG. 2. Power spectral density of OLR during the five months (a)–(h) MJJAS and (i)–(p) NDJFM for the regions (a) Arabian Sea (5°N, 72.5°E), (b) Bay of Bengal (15°N, 87.5°E), (c) South China Sea (15°N, 115°E), (d) Solomon Islands (5°S, 116°E), (e) subtropical central South Pacific (27.5°S, 135°W), (f) eastern North Pacific (15°N, 105°W), (g) Caribbean Sea (30°S, 47.5°W), (h) southeast coast of Brazil (17.5°N, 82.5°W), (i) Zimbabwe (17.5°S, 32.5°E), (j) equatorial eastern Indian Ocean (2.5°S, 90°E), (k) northern Australia (15°S, 130°E), (l) tropical western North Pacific (5°N, 150°E), (m) Samoa (15°S, 170°W), (n) eastern North Pacific (15°N, 115°W), (o) southeast of Brazil (17.5°S, 45°W), and (p) Mauritania (17.5°N, 15°W). The seasonal cycle was removed by applying 121 high-pass filters before the spectrum was calculated. Power spectral density was calculated over a 5° × 5° rectangular box each year and averaged over 27 yr. The smoothed curve is the red noise and the dashed line is the 99% a priori confidence limit.

Objective criteria of the tracking method were used to identify QBW deep convective events by using an OLR anomaly with a 12–20-day bandpass filter applied. The following criteria should all be satisfied for each event: 1) Identify a convectively active region that is enclosed by a $-10$ W m$^{-2}$ contour line at a given time. 2) Its longitudinal scale is more than 15°. 3) Any event should last more than five days. If there is an overlap of contour line of $-10$ W m$^{-2}$ between time t and time $t + 1$, it is considered as a continuous convective system. 4) Minimum

OLR anomaly of the envelope should be below $-20$ W m$^{-2}$ at its mature stage.

The results of the tracking method of course are dependent on the parameters mentioned above; however, sensitivity to the choice of the criteria has been tested and the results are not so sensitive to the selection criteria. At the same time, the selection of the criteria appears valid following the consideration below. 1) The criterion for the convective active region is set to be 10 W m$^{-2}$. From Figs. 3a and 3b, it is seen that the contour lines of 10 W m$^{-2}$ cover most of the regions where the QBW spectral peak is statistically significant (Figs. 3e and 3f). 2) The choice of the longitudinal scale can be validated as follows. Suppose there is a convective anomaly consisting of a monochromatic wave in longitude with 6000-km wavelength, which is a typical zonal scale of observed QBW in the Asian summer monsoon region (e.g., Chen and Chen 1993), and has 15 W m$^{-2}$ in amplitude—considered to be a moderate convective anomaly according to the discussion above, then the longitudinal scale, whose value is less than 10 W m$^{-2}$—a typical OLR STD value as just mentioned above—would be about 15°. 3) Considering the periodicity of QBW, the minimum lifetime of 5 days is reasonable. 4) It seems also reasonable to choose $-20$ W m$^{-2}$, which is twice as large as the typical standard deviation value, as a criterion for mature stage strength.

### *e. EEOF analysis*

The results obtained from the tracking method were further checked by using the EEOF analysis, which enables us to describe a sequence of disturbances in an efficient way (Weare and Nasstrom 1982). The EEOF analysis was applied to the OLR anomaly from $\pm 8$ days with a 4-day time increment. The associated atmospheric motions were obtained by computing lag-regression between horizontal wind anomalies (consisting of zonal and meridional wind components) and the principal components of the EEOF analysis. Associated precipitation anomalies from TRMM 3B42 data were also obtained by the same procedure. Significance of the lag-regression was tested to see whether the null hypothesis that there is no correlation can be rejected. Significance levels were adopted at 95% for winds and 90% for precipitation anomalies, considering the shorter available duration of the precipitation data. Fisher's $z$ transform (a more detailed description can be seen in any statistical text book such as in von Storch and Zwiers 1999) was used in the significance test. To make the results robust, we used the effective number of degrees of freedom (Chen 1982), which takes into account the reduction of degrees of freedom due to the existence of a low-frequency component.

## 3. Geographical distribution of QBW convection

In this section, we offer an overview of the geographical feature of the QBW in terms of its variance. Variance of QBW (Figs. 3a,b) appears to follow the total intraseasonal component (Fig. 1) in both JJA and DJF seasons. For instance, the variance is large in the Asian summer monsoon region in boreal summer. That is the reason why most previous studies have focused on that region. However, in terms of the fractional variance of 12–20- to 20–60- day components, the contribution of the 12–20 day is relatively small where both 12–20-day and intraseasonal variances are large (Figs. 3c,d). The contribution of the 12–20-day component in general is larger in the subtropics and extratropics than in the tropics.

Given that complexity, it is helpful to discuss QBW behavior in terms of signal-to-red noise ratio analysis. Figures 3e and 3f show the geographical distribution of the ratio of the 12–20-day power spectrum density of OLR to the red noise integrated over the same frequency band. The procedure of computing the spectrum density and the red noise is the same as described in the previous section.

Figures 3e and 3f indicate that the most striking feature is that convective activity associated with the QBW is significant in the subtropical regions along 10°–30° latitudinal bands in both hemispheres. This implies that QBW convection has strong impact on the subtropical region rather than the equatorial region. At the same time, QBW convection is suggested, subject to the influences from both tropical and extratropical weather systems. In both seasons, zonal distribution of convective activity does not seem to be symmetric about the equator, but rather shifts slightly to the summer hemisphere. There is also a longitudinal variation. In boreal summer, there is a strong convective activity signal associated with the QBW in the western North Pacific, South China Sea, Southeast Indian Ocean, and the Gulf of Mexico. Moderate signal can be found in the Indian monsoon region, central South Pacific, northern part of Australia, Mozambique, and South America along ~15°S. In contrast, in boreal winter there is a line of significant convective activity across from South Africa to the eastern South Pacific between about 15° and 20°S. A weaker but continuous significant line also can be found in the Northern Hemisphere across from the Arabian Sea to the central North Pacific between about 10° and 20°N. An isolated significant signal can be found in the Caribbean Sea and over South America.

## 4. QBW identified by the tracking method

The tracking method helps display the tendency of the QBW convective anomalies to occur, develop, and dissipate.

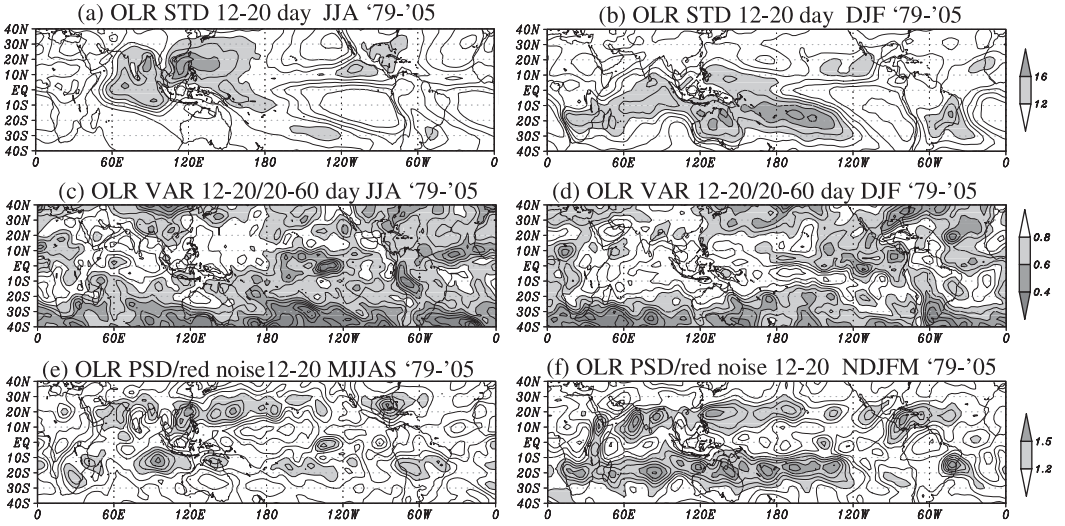


FIG. 3. Geographical distribution of OLR standard deviation of the 12–20-day component for (a) boreal and (b) austral summer and the ratio of 12–20-day variance to 20–60-day variance for (c) boreal and (d) austral summer as well as the ratio of the power spectral density of OLR to red noise integrated over the frequency band corresponding to a 12–20-day period for the (e) extended boreal (MJJAS) and (f) extended austral (NDJFM) summer. Contour intervals in (a) and (b) are 2 W $m^{-2}$; in (c)–(f) 0.1.

### *a. Boreal summer*

The results of the tracking method during boreal summer are shown in Fig. 4. There is a strong concentration of the QBW activity in the South Asian–western North Pacific region indicated by AM (abbreviation for Asian monsoon) in Fig. 4a. Other activity regions can be found in the Central America (CA) region and South Pacific (SP) regions. Two major initial locations can be found, one in the equatorial western Indian Ocean and one in the equatorial western Pacific (Fig. 4b). Some minor initial locations can also be found in the equatorial eastern Indian Ocean, South China Sea, western North Pacific, Caribbean Sea near Cuba, and Uruguay.

After examination of the movement of events that originate from a given location and move to the mature and terminal location (Figs. 4c and 4d), the typical life cycle of the QBW events could be inferred (indicated by thick arrows in Fig. 4c). In the AM region, many events tend to be initiated in the equatorial western Pacific and move northwestward. Most of them tend to move farther westward and reach the South China Sea, but some tend to turn northeastward and dissipate in the western North Pacific. Some of the convective events that reached the South China Sea tend to dissipate there and some tend to reach the Indian Ocean where they tend to merge with the convective events originated in the Indian Ocean. In contrast, most convective events that originate in the Indian Ocean tend to converge in the equatorial western Indian Ocean with some in the equatorial eastern Indian Ocean. The convective activity that occurred in the equatorial western Indian Ocean tends to move eastward along the equator. On its way, some convection tends to move northward or northwestward into the Arabian Sea or Bay of Bengal and some turns southward into the south Indian Ocean. A detailed description will be made using the EEOF analysis in section 5.

Convective activity in the SP region appears to be simpler. Almost all events tend to emerge in the equatorial western Pacific, move southeastward, and dissipate in the central South Pacific. The convective activity over Brazil tends to move a little northeastward. There is an indication of the connection between the convective activity originating in the equatorial western Pacific and that over Brazil (Fig. 4a)—to be discussed in section 5.

In Central America, most convective events occur in the Caribbean Sea near Cuba and move westward crossing Mexico. They finally reach the eastern North Pacific and tend to dissipate there.

### *b. Austral summer*

A variety of the QBW events exists in austral summer (Fig. 5). Most occur in the Australia monsoon–South Pacific convergence zone (SPCZ) region. One major track of convective events of the QBW emerges over South Australia and moves northeastward, where some dissipate over the northeast coast of the continent and others reach the western South Pacific. Another major track is that of convection emerging in the western South Pacific somewhere east to New Guinea and moving

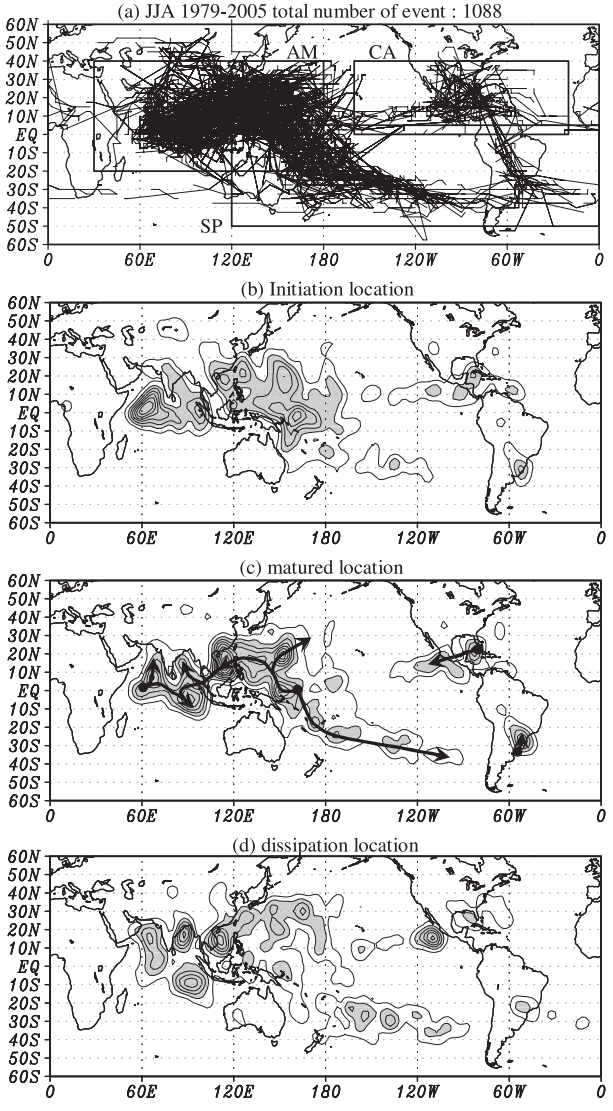


FIG. 4. The QBW events identified by the tracking method for JJA: (a) spaghetti diagram and contour plots of (b) initial, (c) mature, and (d) termination location. Contour intervals are 0.2; values greater than 0.4 are shaded. Arrows in (c) highlight the propagation paths tracked.

eastward/southeastward and dissipating in the eastern South Pacific.

There are other QBW events around the globe. One event lies in the North Pacific (NP) in which convection tends to move northwestward in the western NP and eastward in the eastern NP. Eastward-propagating convective events are suggested to exist in the South Africa–south Indian Ocean (SAf) region and North Africa–North Atlantic (NAf) region. Southeastward- and northeastward-propagating convective events are suggested to be present in the Indian Ocean and South America–South Atlantic (SAm) region, respectively.

## 5. Life cycle of the QBW revealed by EEOF analysis

We next describe the detailed behavior of QBW events by means of the EEOF analysis introduced in section 2e. As stated earlier, the EEOF analysis was performed from −8 day to +8 day with 4-day increments. At a first glance of the EEOF results, one would notice that the horizontal patterns of both the convective anomaly and the wind anomaly at day −8 are quite similar to those at day 8. Thus, the EEOF results from day −8 to day 8 represent one averaged cycle of the QBW events, so the periodicity of the QBW events is considered to be ~ 16 days—a result of the spectral filtering. In the end, we will show that the results presented here are in good agreement with the results obtained in the previous section (tracking method).

### *a. Boreal summer QBW life cycle*

#### 1) ASIAN MONSOON REGION (AM MODE)

First, we focus on the AM region (Fig. 6) in which QBW events are highly concentrated during boreal summer (Fig. 4). A convective anomaly emerges in the equatorial western Pacific at day −4 and moves westward along the equator with development by day 0. Then it starts to move northwestward by day 4. At day 4 a Rossby wave response appears in both hemispheres with a stronger northern branch. Note that the center of vorticity in the northern branch is located northwest of the center of the convective anomaly. The convective anomaly reaches its mature phase over the South China Sea at day 8 (also day −8), consistent with the results suggested with the tracking method (Fig. 4c). By this time, a clear double-cell cyclonic circulation whose center is located around 10°N is formed, which is in good agreement with previous studies (e.g., Chen and Chen 1993). Another essential correspondence with previous studies is the horizontal scale and phase speed of the disturbance. The zonal wavelength is roughly estimated as 70° longitude and the westward phase speed is about 6 m $s^{-1}$, which are consistent with previous studies (e.g., Chen and Chen 1993). Four days later (at day −4) the convective activity weakens and reaches the Indochina Peninsula. At the same time, there is a small convective anomaly to the northeast that splits from the main body. This is also consistent with the tracking method in that there is a trend of convective activity to move northeastward in the western North Pacific. Also at day −4, a convective anomaly starts to emerge in the equatorial western Indian Ocean, which is one of the major initial locations in this season (Fig. 4b). This convective anomaly appears to be related to the cyclonic circulation of the southern branch of the double cell. Two convective anomalies, one originating

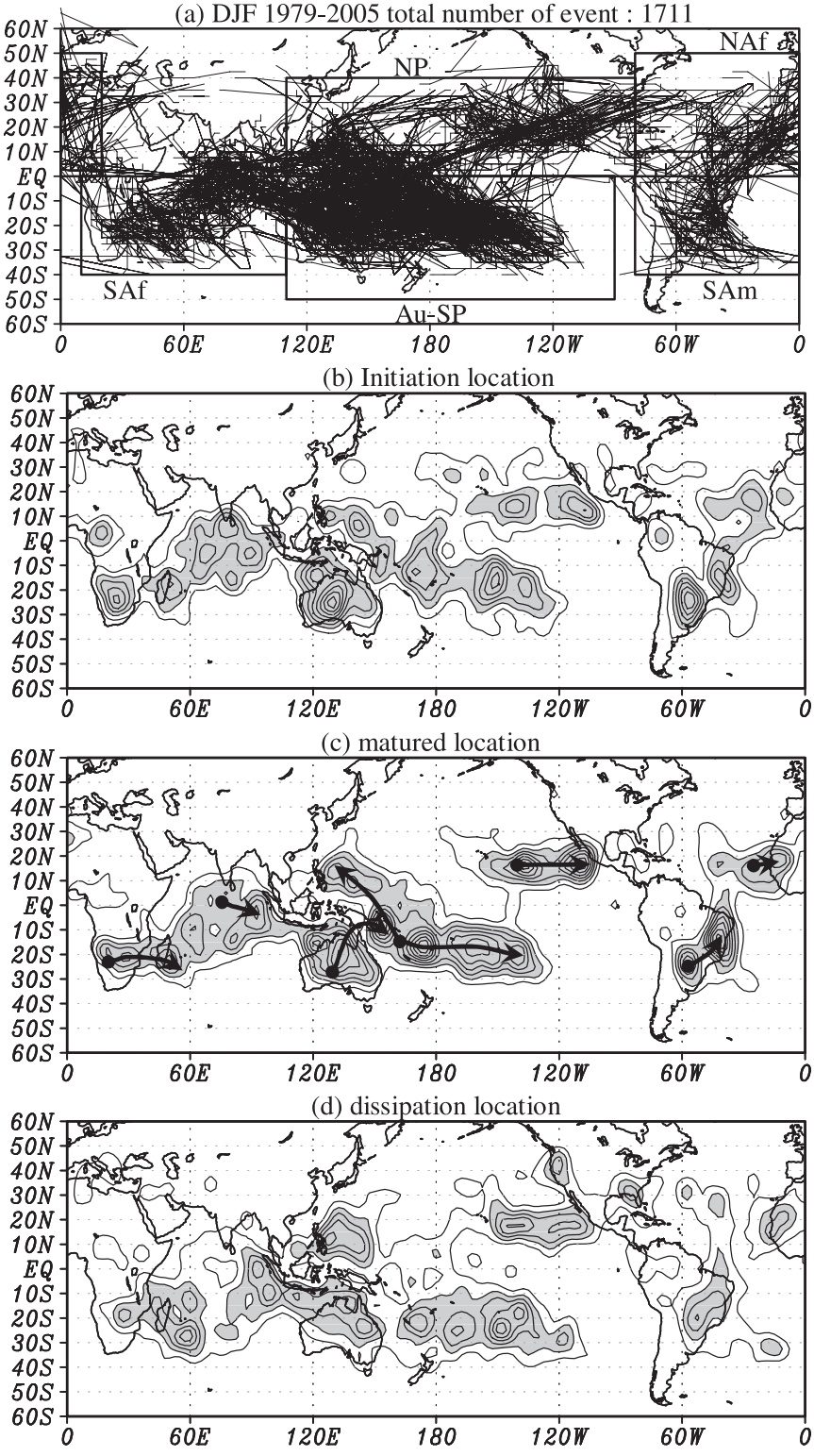


FIG. 5. As in Fig. 4 but for DJF.

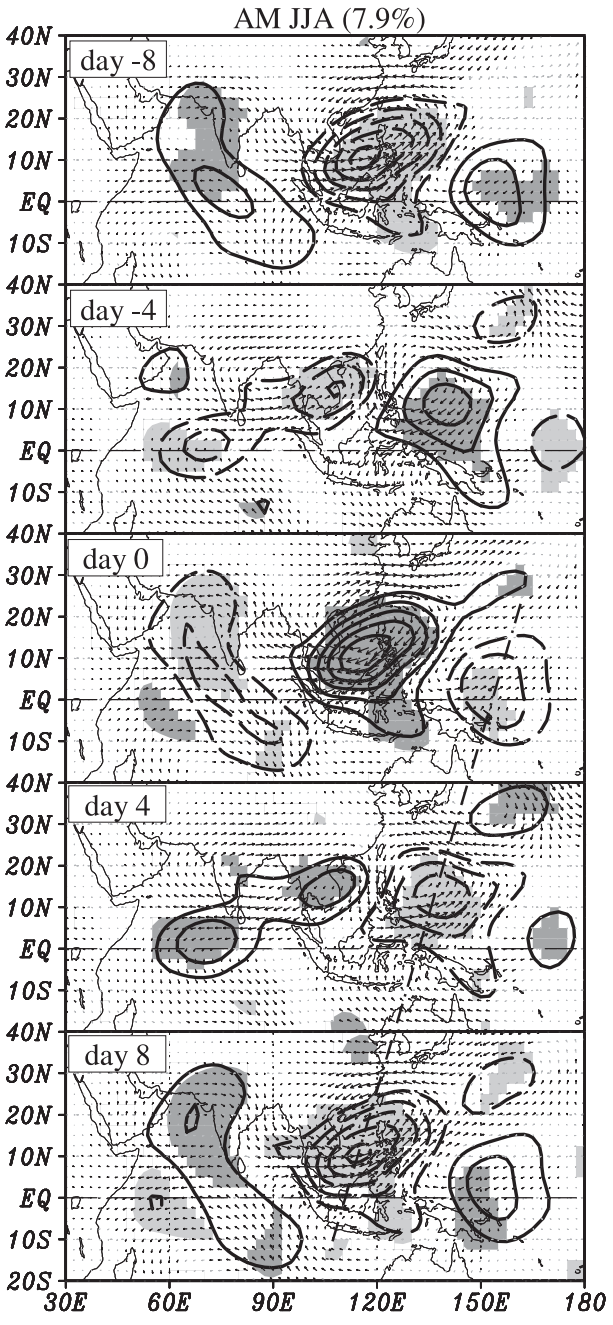


FIG. 6. Life cycle of the summer QBW in the AM region represented in terms of $EEOF_1$ applied to the 12–20-day bandpass-filtered OLR anomaly (contours) with five time lags from −8 to 8 day using 4-day time increments. Lag-regression was used to obtain 850-hPa wind fields (vectors) and TRMM 3B42 precipitation (shades). Contour intervals of OLR anomaly are 0.01. Thick vectors represent significant winds (either zonal or meridional wind) at the 95% level and shades represent precipitation anomaly significant at the 90% level. The thick dash–dotted line is drawn referenced to the propagation of a convective anomaly.

in the equatorial western Indian Ocean and the other traveling from the western Pacific, merge by day 0 making a northwest–southeast slantwise convective band in the Indian Ocean. An interesting feature is that the double cell also has a slantwise structure like the convective anomaly. This is the last time that the convective anomaly is traced, thus the Arabian Sea and the central south Indian Ocean are considered one of the common dissipation locations, which is quite consistent with the results derived from the tracking method (Fig. 4d). Also, note that the OLR anomalies (contours) are a good proxy of precipitation anomalies (shades).

As mentioned in section 2, there are relatively many observational studies focused on this area in this season. This study, however, provides revealing evidence in the QBW life cycle by use of a long-term composite and two methods. Most of the previous studies (e.g., Chen and Chen 1993, 1995) except Mao and Chan (2005) are based on case studies. Essentially the life cycle of QBW convection and its relation to low-level circulation in this study seems to be consistent with the composite study of Mao and Chan (2005). One major finding in this study is that QBW convection emerges in the equatorial western Indian Ocean as well as the equatorial western Pacific. Although the mechanism is unclear, both the tracking method and EEOF analysis support this novel finding, and this phenomenon is probably important in initiating or enhancing QBW convection in the Indian monsoon region.

### 2) CENTRAL AMERICA (CA MODE)

Next we look at the Central America region where QBW events tend to occur often (Fig. 4a). A small convective anomaly emerges in the central tropical Atlantic Ocean at day −8, as shown in Fig. 7. Northwestward propagation is suggested from the ensuing locations. At day 0 the convective anomaly reaches its mature stage over the Caribbean Sea. A cyclonic circulation anomaly associated with the convective anomaly is established to the northwest of the convective anomaly by this time. An interesting feature is that an anticyclonic circulation anomaly exists to the north but not to the south of the cyclonic circulation. Why the anticyclonic circulation anomaly appears to the north and how it affects the cyclonic circulation anomaly are not obvious, but this interesting feature to note is different from the case in the AM region. From day 0 on, it continues to move westward with the cyclonic circulation anomaly remaining to the northwest by day 8. It finally disappears in the eastern Pacific at day −4. The life cycle is also consistent with the result suggested by the tracking method (Fig. 4c).

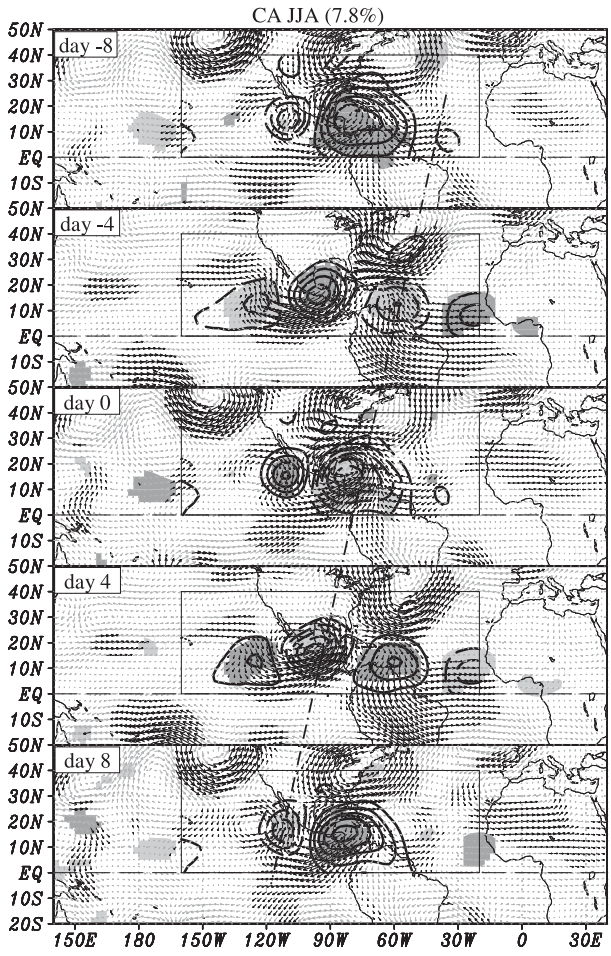


FIG. 7. As in Fig. 6 but for the Central America region. Solid box represents the region for which EEOF analysis was performed. The thick dash–dotted line is drawn referenced to the propagation of a convective anomaly.

Also note the similarities between the CA and AM mode. The wavelength of the convective anomaly of the CA mode is about 70° of longitude (which is relatively clear at day −4 in Fig. 7), similar to the horizontal scale of the westward-propagating disturbance of the AM mode. In addition, its phase speed of about 5 m $s^{-1}$ is also close to that of the westward-propagating AM mode.

#### 3) SOUTH PACIFIC REGION (SP MODE)

Prominent Rossby wave trains appear in the South Pacific extending from New Guinea to southern Brazil (Fig. 8). The zonal wavelength of the wave trains is about 60° of longitude and the wave train propagates eastward at a speed of ~5 m $s^{-1}$. The relationship between the convective anomalies and the horizontal winds follows what is suggested by the quasigeostrophic theory; that is, the convective anomalies coincide with northerlies and the suppressed convection coexists with southerlies. It is beyond doubt that the OLR anomalies represent precipitation anomalies very well.

### *b. Boreal winter QBW life cycle*

#### 1) AUSTRALIA–SOUTH PACIFIC (AU–SP MODE)

The convective anomaly over Australia is characterized by Rossby wave trains (Fig. 9). The zonal wavelength is about 50° of longitude and the convective anomaly propagates northeastward at a zonal speed of ~4 m $s^{-1}$. The convective activity and circulation anomaly are clearly connected. This pattern suggests an incoming Rossby wave train from the southwest, especially at day 0 when the convective anomaly is initiated over the southwestern part of Australia, which is one of the major initiation locations in this season (Fig. 5b).

On the other hand, the convective activity of the QBW in the tropical South Pacific appears to show a somewhat different propagation characteristic. When it reaches the western South Pacific, it fully develops (day 8) and moves eastward, instead of northeastward, at ~ 6 m $s^{-1}$, a little bit faster than over Australia, and finally disappears in the eastern South Pacific at day 0. The relationship between the convective anomaly and the circulation anomaly is also clear and similar to that over Australia: the convective anomalies are associated with the northerly wind anomalies.

#### 2) SOUTH AFRICA–SOUTH INDIAN OCEAN (SAF MODE)

The incoming extratropical Rossby wave is suggested to play a role in initiating QBW convection in the South Africa–south Indian Ocean region (Fig. 10). Two convective anomalies emerge at −8 day. One is over Botswana; the other in the central Indian Ocean. Associated Rossby wave trains can be clearly seen and also can be traced farther southwest in the EEOF analysis domain. The two convective anomalies show different propagation characteristics. The convective anomaly located over Botswana moves northeastward with zonal phase speed of ~5 m $s^{-1}$ and that in the central Indian Ocean moves southeastward from day −8 to −4. Why do they show different propagation characteristics? This can be attributed to the fact that the equatorial anomaly is associated with an equatorial Rossby wave, while the subtropical anomaly is an extratropical Rossby wave. They might originally be initiated by the same incoming extratropical Rossby wave train, but the subsequent behavior might be different. They finally merge in the western south Indian Ocean at day 0. The merged convective anomaly then moves eastward and disappears over the central south Indian Ocean at day 4.

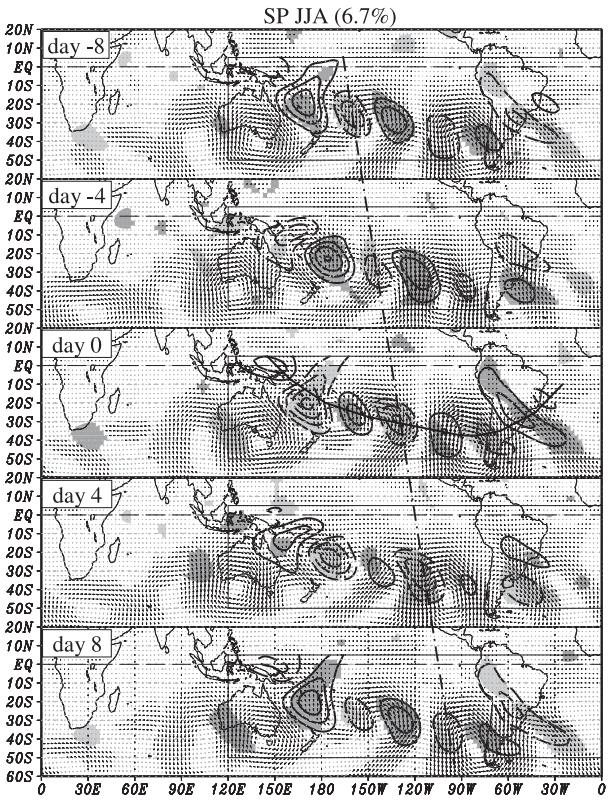


FIG. 8. As in Fig. 7 but for the South Pacific (SP) region. Thick solid curve is drawn in reference to wave trains referred to in Fig. 14.

### 3) NORTH PACIFIC (NP MODE)

A convective anomaly emerges in the equatorial western Pacific at day 4 (Fig. 11). Associated cyclonic circulation anomalies are accompanied in both hemispheres with a stronger northern branch. This structure is consistent with composite results of QBW oscillation in the previous studies in the Pacific in austral summer (e.g., Kiladis and Wheeler 1995; Chatterjee and Goswami 2004). The convective anomaly moves northwestward and reaches the western Pacific north of New Guinea at day 8 and intensifies, consistent with the results obtained with the tracking method (Fig. 5c). After four days (day −4), the convective anomaly in the western North Pacific splits with one center weakening and moving northwestward and another center occurring in the central North Pacific. The weakening center is associated with a cyclonic circulation anomaly. The genesis center is located to southwest of an anticyclonic circulation anomaly. The new convective anomaly moves eastward by day 4, then dissipates off the coast of Mexico.

The life cycle inferred from the tracking method (Fig. 5c) suggests that two different modes occur in the NP region: one occurs in the western North Pacific and the other in the eastern North Pacific. The EEOF result suggests that they are related. This discrepancy deserves further study. One possible reason is that the WNP oscillation has large variance of 20–25 days while the eastern North Pacific has large variance of 12–18 days (Figs. 2l and 2n). A uniform 12–20-day filter was applied to the entire region, thus the signals may be distorted. An interesting feature is that they show quite different characteristics in both propagation and structure. The former appears to be associated with the equatorial Rossby wave, and the latter with the extratropical Rossby wave in terms of of propagation and structure characteristics. The connection between these two modes will be discussed in more detail in section 6b.

### 4) NORTH AFRICA–NORTH ATLANTIC (NAF MODE)

An incoming Rossby wave seems to be a major player in QBW events in the North Africa–North Atlantic sector, too. A convective anomaly emerges in the Atlantic Ocean to the northeast of Venezuela at day −8 (Fig. 12). Wave trains can be easily identified at this time, associated with convective anomalies; the northerly (southerly) wind anomalies are associated with negative (positive) convective anomalies. The convective anomaly at day −4 is located in the United States east of Charlotte, North Carolina, and is still associated with a southerly wind anomaly, which is part of the wave train. The convective anomalies described above do not appear to be a major mode in this region, partly because they are little recognized by the tracking method (Fig. 5) and partly because their amplitude is small. The major mode appears as a significant development of convection in the eastern North Atlantic Ocean at day 0. Similar but opposite in sign to day −8, there are clear wave trains in the EEOF domain. The large convective anomaly is also associated with a northerly wind anomaly of a cyclonic circulation in the wave trains. Four days later (day 4), the convective anomaly disappears over North Africa. The life cycle presented here is consistent with the result of the tracking method (Fig. 5) in that the convective anomaly emerges in the eastern Atlantic Ocean, moves eastward, and dissipates over North Africa. A minor difference is that the major dissipation area of the tracking method seems to be a little westward, which is probably attributed to the sensitivity to the selected criteria of the tracking method.

### 5) SOUTH AMERICA–ATLANTIC OCEAN (SAM MODE)

Rossby wave trains also seem to initiate QBW convection in the SA region (Fig. 13). A convective anomaly associated with the northerly wind of an anticyclonic

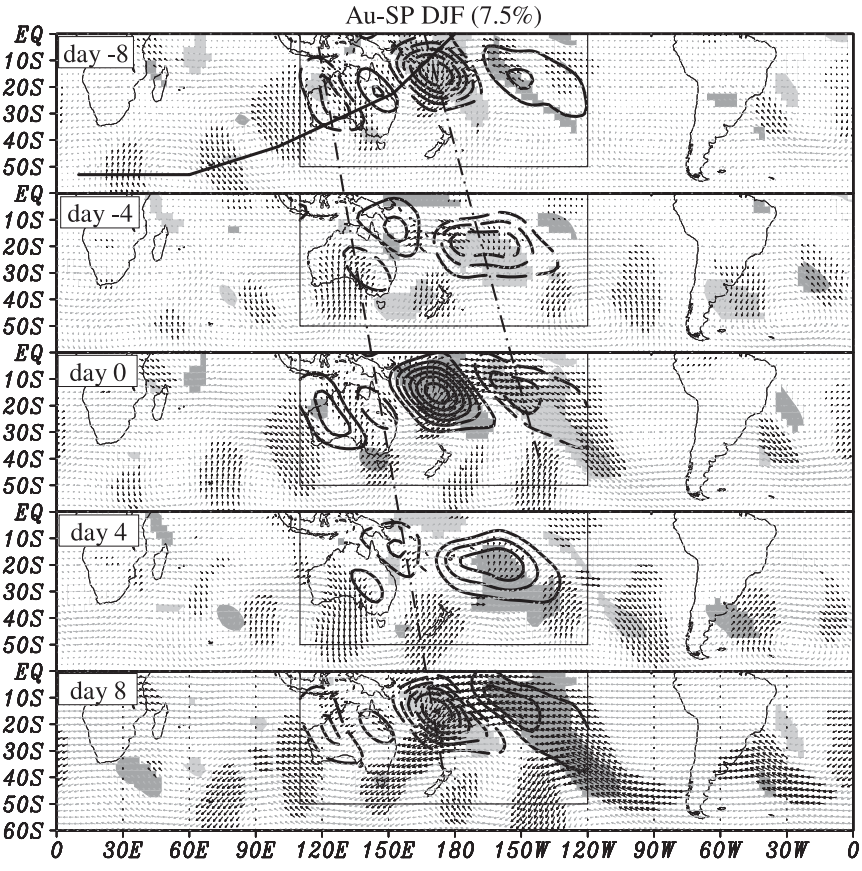


FIG. 9. As in Fig. 8 but for the Australia–South Pacific region during austral summer.

circulation anomaly emerges over Paraguay at day 0. The convective anomaly moves eastward by day 4. At this time, the convective anomaly accompanies a cyclonic circulation anomaly, but is still associated with a northerly wind anomaly. Then it moves northward to the equator by day 8 when it reaches its mature phase. This track is consistent with the results obtained from the tracking method (Fig. 5c). It finally dissipates north of the equator at day −4.

#### 6) INDIAN OCEAN REGION

Last, we mention QBW convection in the tropical Indian Ocean (the rectangular area 15°N–15°S, 50°–120°E). Since this mode is weak and peculiar, we only briefly mention it. The EEOF analysis indicates the convective activity, having eastward propagation (not shown), is consistent with the results deduced from the tracking method (Fig. 5). However, it is hard to find good correspondence between the circulation anomaly and any equatorial waves. Given the presence of rotational flow across the equator, mixed Rossby gravity wave might be one of the best candidates. The ambiguous structure probably attributes to the fact that the disturbance there is not very significant in terms of spectral filtering (e.g., Figs. 2j and 3f); namely, QBW events there are more a random stochastic event rather than a periodic phenomenon.

## 6. Origin of the QBW mode

Examination of the EEOF patterns suggest that QBW are closely associated with the westward propagation of equatorial Rossby waves and the eastward propagation of extratropical Rossby wave trains.

### *a. Equatorial Rossby waves*

The connection between the QBW systems and equatorial Rossby waves seems to be well recognized but remains controversial in some aspects. Chen and Chen (1993) revealed QBW structure and propagation characteristics based on the 1979 summer monsoon. They showed that the QBW in the Indian Ocean have a double-cell with one cell centered at about 15°–20°N and the other at the equator, which does not fit in the

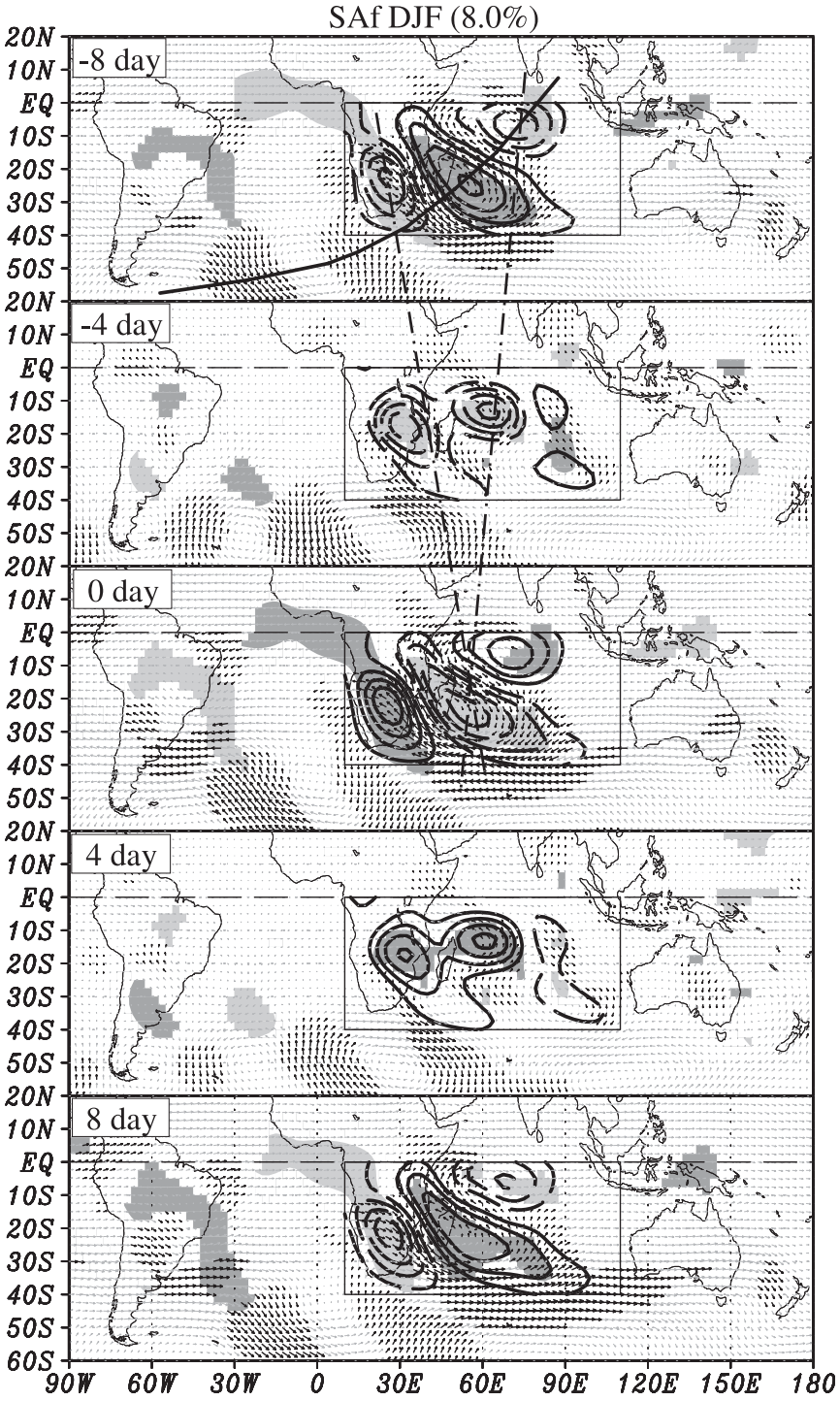


FIG. 10. As in Fig. 9 but for the South Africa–south Indian Ocean region.

structure of an equatorial Rossby wave in the absence of background flow (Matsuno 1966). Based on the Tropical Ocean and Global Atmospheric Coupled Ocean–Atmosphere Response Experiment (TOGA COARE) results, Numaguti (1995) detected a 15–20-day oscillation with zonal wavelength of about 6000–8000 km and westward propagation of about 4–5 m $s^{-1}$ during austral summer and concluded that the QBW can be

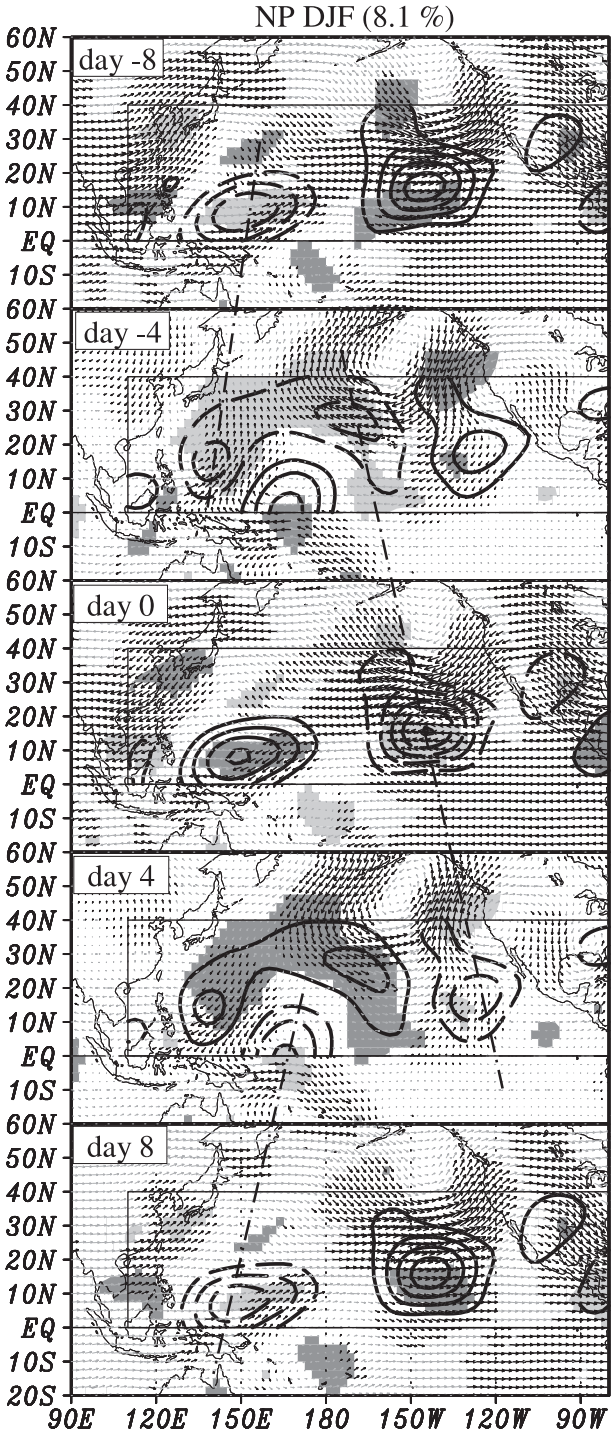


FIG. 11. As in Fig. 9 but for the North Pacific region.

interpreted as an $n = 1$ equatorial Rossby wave in terms of the structure and phase speed. Kiladis and Wheeler (1995) further described the behavior of the equatorial Rossby waves using 8 years of austral summer data and showed that the characteristics of the equatorial Rossby waves that they examined are consistent with Numaguti's (1995) finding. However, at the same time they pointed out the behavior of the equatorial Rossby waves cannot be accounted for by linear Rossby wave theory, even taking into account the effect of basic zonal flow in terms of vertical structure, phase speed, and group velocity. Chatterjee and Goswami (2004) mentioned the universality of the QBW structure between boreal and austral summer. They made a composite for both boreal and austral summers and suggested that the northward (southward) shift of cyclonic pairs during boreal (austral) summer is due to the shift of a dynamical equator, that is, the zero ambient absolute vorticity line.

For interpretation of the behavior of the QBW mode, it is useful to note that the atmosphere has complex three-dimensional basic flows and strong convection–circulation coupling, which can significantly, and sometimes drastically, modify the behavior of dry (Wang and Xie 1996) and moist (Xie and Wang 1996) equatorial Rossby waves. From the similarities in structure between the QBW behaviors in this study and the previous studies (e.g., Chatterjee and Goswami 2004), during boreal summer the AM and CA modes (Figs. 6 and 7) are likely manifestation of the moist equatorial Rossby waves modified by the climatological mean flow. During austral summer, the tropical convection parts of the SAf and NP modes have a horizontal structure resembling equatorial Rossby waves (Figs. 10 and 11). The common feature of these disturbances is westward/northwestward (westward/southwestward) propagation in the Northern (Southern) Hemisphere. Another common feature is the easterly vertical shear in background. Wang and Xie (1996) and Xie and Wang (1996) investigated the effect of vertical shear on equatorial waves and concluded that easterly shear provides a preferable condition for unstable Rossby waves. The strong easterly vertical shear also provides a mechanism for steering Rossby wave poleward (Jiang et al. 2004; Drbohlav and Wang 2005). In fact, the strong easterly shear lies in the Asian monsoon region extending from the northern Indian Ocean to the western North Pacific during boreal summer. At the same time, the CA region has weaker easterly vertical shear associated with the North American summer monsoon. On the other hand, the tropical Indian Ocean and western Pacific have such easterly vertical shear during austral summer. The westward and poleward propagation of the AM, CA modes during boreal summer, and the SAf and NP modes during austral summer of QBW convection therefore appear to be associated with equatorial Rossby waves.

The basic effect of the background vertical shear on the equatorial Rossby wave can be discussed in terms of

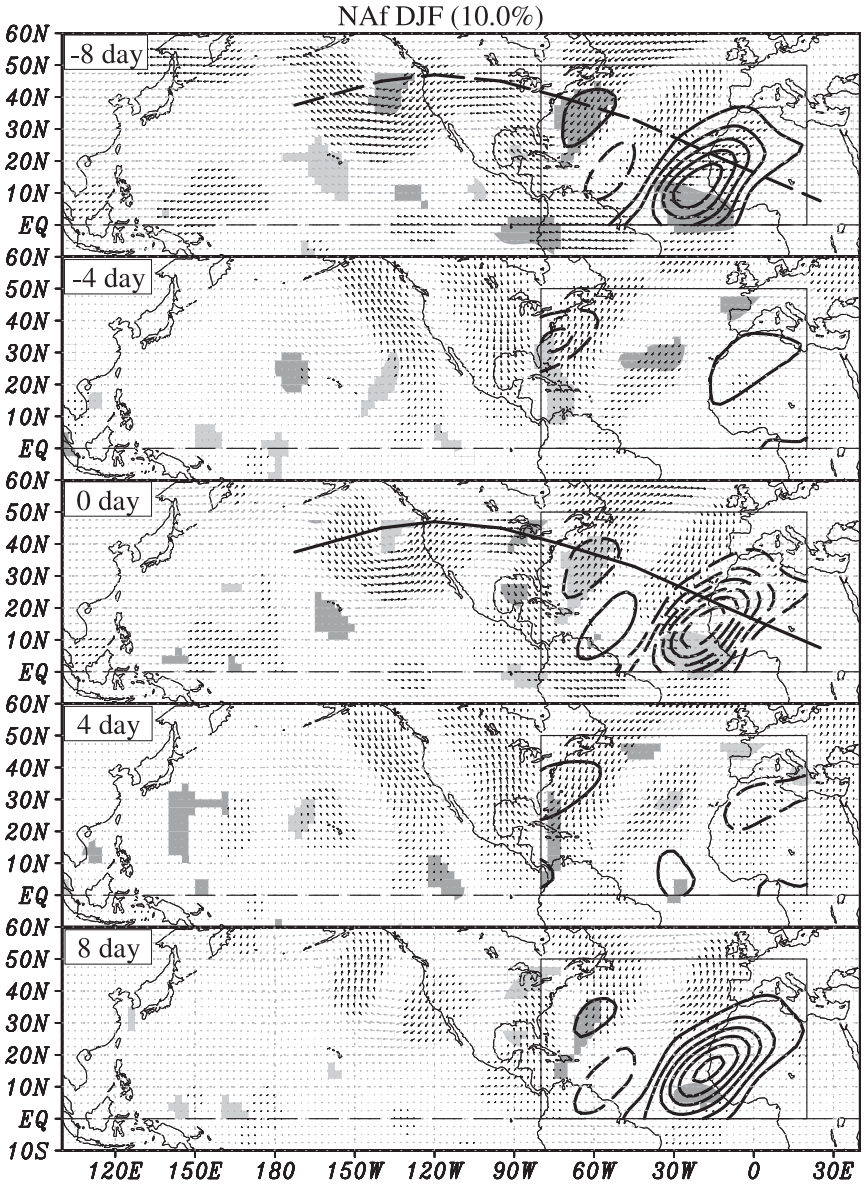


FIG. 12. As in Fig. 9 but for the North Africa–North Atlantic region.

the climatological field; however, a more complete description needs further consideration of lower frequency components such as the MJO and El Niño–Southern Oscillation (ENSO). The background that affects the activity of QBW is considered as the sum of the climatological circulation plus MJO/ENSO-related circulation anomalies. In the region where climatological vertical shear is weak, the MJO/ENSO-related vertical shear effects could be dominant. A couple of recent studies suggest evidence that the activity of QBWs is modulated by lower frequency components in some regions. Yang et al. (2008) showed that the activity of QBW modes that influence the South China Sea, originating from the equatorial western Pacific (which corresponds to the AM mode in our study), can be significantly modulated by the change of background state there on interannual and interdecadal time scales. Other evidence was shown by Wu et al. (2009) that a 10–15-day time-scale system in the Central America region (which corresponds to the CA mode in our study) tends to be modulated by the MJO. This topic is of course beyond the scope of this study; however, it would be a promising topic in terms of multiscale interaction.

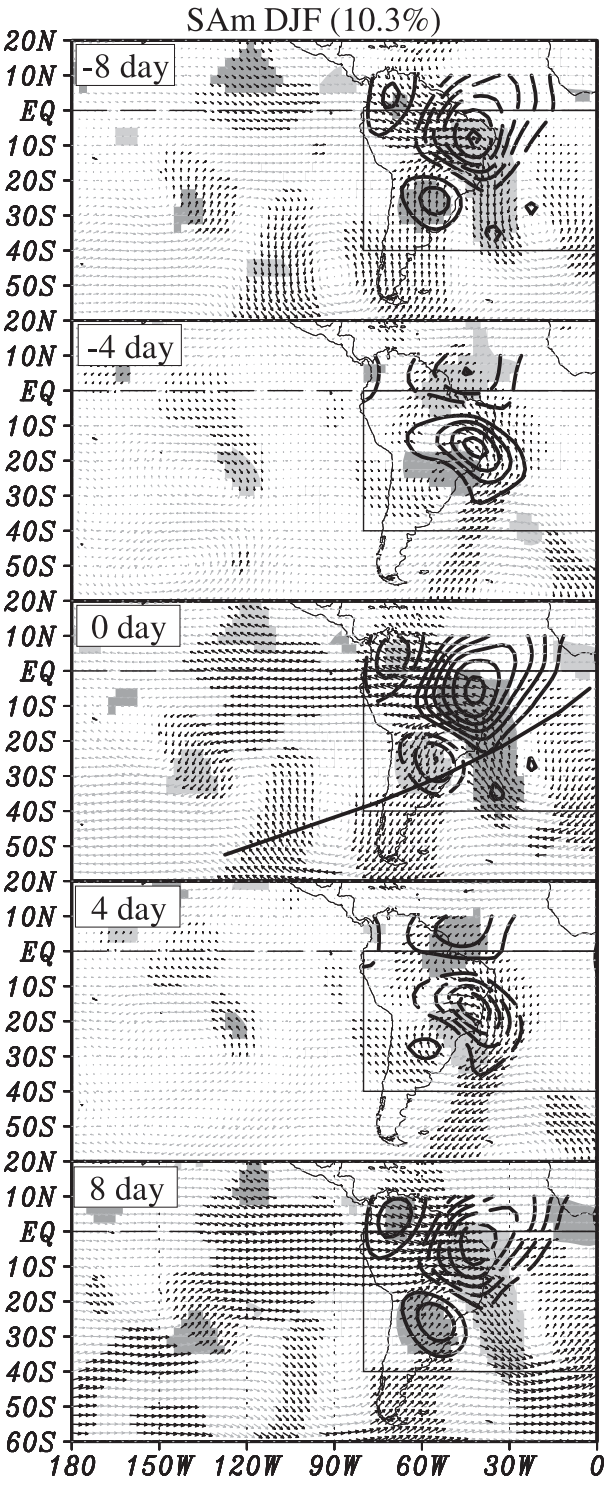


FIG. 13. As in Fig. 9 but for the South America–Atlantic Ocean region.

*b. Rossby wave trains*

As we have seen in the previous section, the connection exists between Rossby wave trains and QBW convection in several regions where the Rossby wave trains can be traced farther to the west of the QBW convection. These wave trains follow a great circle route as shown in Figs. 8–10, 12, and 13. These figures provide evidence that incoming Rossby wave trains maintain the QBW convection in some ways in terms of its initiation and/or development. In fact, there is evidence that supports incoming extratropical Rossby waves inducing tropical convection on a similar but broader (submonthly, 6–30 day) time scale (Kiladis and Weickmann 1992, 1997; Tomas and Webster 1994). Theoretical study suggests that Rossby waves are able to penetrate into the tropics in the region of upper-tropospheric westerlies (Webster and Holton 1982). In fact, the regions where incoming Rossby wave trains are suggested in the previous section have upper-level westerlies (not shown). Those regions also correspond well to those suggested by theoretical study as preferred locations for incoming Rossby waves, on the basis of stationary wave consideration during boreal winter (Fig. 13 of Hoskins and Ambrizzi 1993).

To develop our understanding of the relationship between Rossby wave trains and QBW convection we further examine the vertical structure of Rossby wave trains. Figure 14 shows the longitude–height cross section of the relative vorticity anomaly along the path of the wave trains shown in Figs. 8–10, 12, and 13. In almost all cases, Rossby wave trains virtually have barotropic structure in the troposphere. Slight westward tilt with height below 700 hPa can be seen in some cases. A common feature to note is that convective anomalies are associated with low-level northerly (southerly) wind anomalies in the Southern (Northern) Hemisphere, which can also be seen in the EEOF figures we examined in section 5. The relationship between convective anomalies and vortices is thus consistent with the structure implied by the quasigeostrophic theory.

To make the result more robust, a teleconnectivity map (Wallace and Gutzler 1981) during boreal winter is shown in Fig. 15. It is easy to find good correspondence between the incoming Rossby waves and the teleconnectivity pattern. The location and zonal scale between them appears consistent. For instance, there is a strong connectivity in the south Indian Ocean to the south of Australia corresponding to the Au–SP mode, in the South Pacific–South America corresponding to the SAm mode, in the South Atlantic corresponding to the SAf mode, and three consecutive patterns in the North America–North Atlantic corresponding to the NAf mode. In addition, it is important to note that there is strong connectivity between the Korean Peninsula and central North Pacific. In our Fig. 11 at day −4, there is a discernible cyclonic circulation anomaly near Okinawa

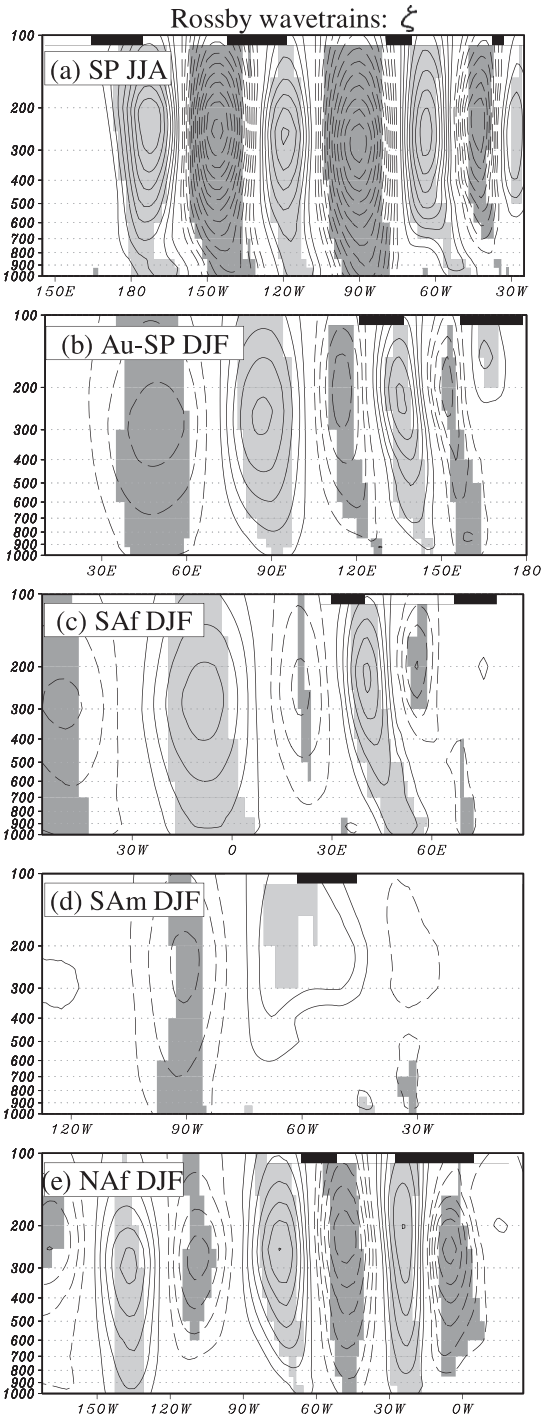


FIG. 14. Vertical structure of relative vorticity associated with Rossby wave trains that affects QBW convection. The abscissa indicates longitude. The section in each panel is along the corresponding curve shown in Figs. 8–10, 12, and 13. Contour intervals are $5 \times 10^{-7}$ s$^{-1}$. Shading shows significance at the 95% level. The thick lines at the top of each figure indicate the existence of convective anomalies that correspond to the first negative contours of OLR anomaly in Figs. 8–10, 12, and 13.

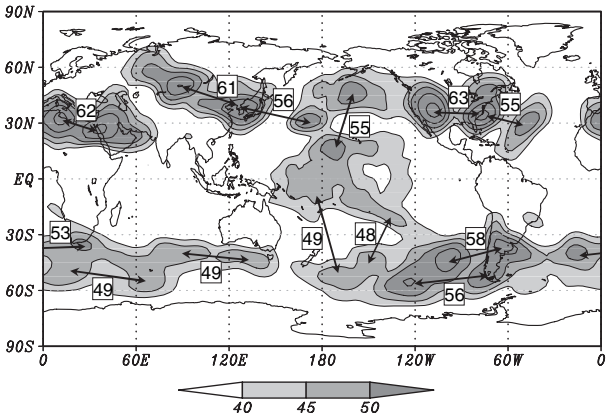


FIG. 15. Teleconnectivity of the 500-hPa geopotential height anomaly of the 12–20-day component during austral summer. Arrows indicate a strong negative simultaneous correlation. Numbers adjacent to arrows represent the correlation coefficient (multiplied by −100) between two regions.

and an anticyclonic circulation anomaly in the central North Pacific. The relative relationship between them appears to be consistent with the teleconnectivity map (Fig. 15). It is thus speculated that, when the convective anomaly accompanying the cyclonic circulation anomaly associated with equatorial Rossby wave, discussed in the previous subsection, reaches the Philippine Sea, it induces an anticyclonic circulation anomaly in the central North Pacific that is responsible for eastward-propagating convective anomaly in the central-eastern North Pacific through Rossby wave trains.

Finally, the propagation behavior of incoming Rossby wave trains is briefly discussed in terms of barotropic Rossby wave theory. The dispersion relation for a barotropic Rossby wave is given by (e.g., Hoskins and Ambrizzi 1993)

$$\omega = \bar{U}k - \beta_* k/\mathrm{K}^2,$$

where $\bar{U}$ is the basic zonal flow, $\beta_* = \beta - \partial^2\bar{U}/\partial y^2$ is the meridional gradient of absolute vorticity, and $K = (k^2 + l^2)^{1/2}$ is the total wavenumber. Suppose we look at the Au–SP mode during austral summer: the zonal wavelength is 50° and meridional wavelength 40°, $\bar{U} =$ 10 m s$^{-1}$, and $\beta_* = 2 \times 10^{-11}$, then the zonal phase speed $c$ becomes 4 m s$^{-1}$, which is consistent with the zonal phase speed of the convective anomaly (Fig. 9). Similar calculations can be applied to other regions where QBW convection is affected by Rossby wave trains and the observed speeds are also consistent with theoretical estimates. In conclusion, the Rossby wave trains probably play an important role in controlling the QBW convection in terms of both initiation and development.

## 7. Summary

Two different methods provide quite consistent features of the life cycle of the QBW in terms of initiation, development, and dissipation. Both methods, of course, are dependent on some parameters, for instance, the threshold OLR value or longitudinal scale for the tracking method and the selected domain, maximum lag, and time increment for the EEOF analysis. As to the tracking method, the number of events, thus the number of initiation, matured, dissipation events changes with the tracking parameters. However, the overall characteristics—namely the tendency of initiation, development, and dissipation—are little affected as many sensitivity tests suggested. As to the EEOF analysis, we have carefully chosen the domain for the analysis based on the results of the tracking method. The results presented in this study are our results after we did several trials with changing the domains to ensure that our results are robust.

The use of TRMM 3B42 precipitation data adds reliability to our results. Although the duration of the TRMM 3B42 data (8 yr) is short compared to that of OLR, it ensures that almost all convective signals implied by OLR indeed accompany precipitation anomalies. The tracking method, which completely relies on OLR fluctuations, is thus considered to provide reasonable descriptions of QBW convection.

It is suggested that QBW convection in some areas is strongly associated with equatorial Rossby waves, not only with the Asian monsoon (Fig. 6) and North Pacific (Fig. 11) modes examined in previous studies (e.g., Chen and Chen 1993; Numaguti 1995), but also with other modes such as the Central America and South Africa–south Indian Ocean modes. The propagation of such convection is characteristically westward with some poleward component.

In addition, extratropical Rossby waves play an important role in maintaining QBW convection in some regions. The Rossby wave trains have virtually barotropic structure and trigger subtropical QBW convection. The propagation of QBW convection associated with Rossby wave trains is eastward and equatorward.

Geographical distribution of power spectrum density (Fig. 3) shows that convective activity associated with the QBW is predominant in the off-equatorial region between 10° and 30° latitude in both hemispheres. The circulation systems there are affected by both tropical and extratropical influences. QBW convection is therefore affected by both equatorial and extratropical Rossby waves.

The result of this study provides a schematic diagram of QBW systems in the tropics (Fig. 16). Since most studies have primarily focused on the QBW behavior in the Asian monsoon region. The observational evidence in this study is largely new and should encourage further studies to elucidate the complex QBW behavior in the entire tropics; this is mandatory for our thorough understanding of complicated tropical weather and intraseasonal variations. One attractive example of future targets is its relation to tropical cyclones. Some equatorial wave types are known to play a significant role in cyclogenesis; the equatorial Rossby wave is one of them (e.g., Frank and Roundy 2006). As we showed, some QBW modes are associated with equatorial Rossby waves: Thus, some QBW modes might be related to tropical cyclogenesis. In fact, the QBW pattern in terms of OLR and low-level circulation appears to be quite similar to the composite of Frank and Roundy (2006) in the AM and CA modes. Further studies thus will be needed to elucidate the behavior of QBW, which leads to the development of not only the QBW itself but also complicated tropical weather systems including tropical cyclones and monsoon depressions.

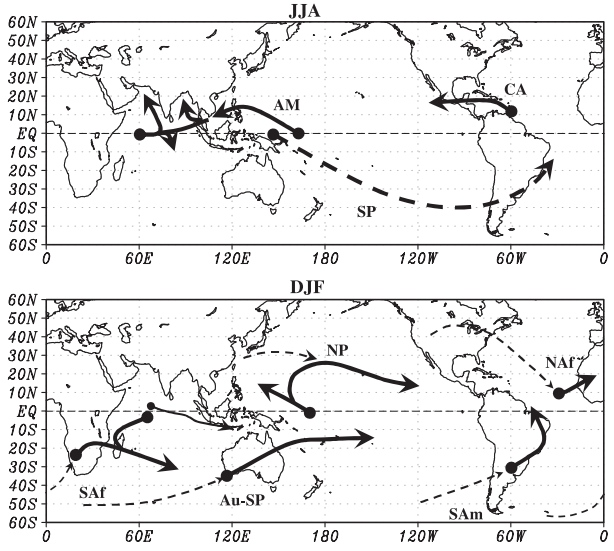


FIG. 16. Schematic summary of the life cycle of QBWs based on results of the EEOF as well as the tracking method. Solid arrows indicate propagation of convection anomalies associated with the QBW. Thick dotted line indicates apparent propagation of equatorial Rossby waves or the Rossby wave train that induces QBW convection. Thin dotted lines indicate the possible Rossby wave train intrusion that is probably responsible for the maintenance of QBW convection. Thin arrow represents QBW convection in the tropical Indian Ocean during austral summer (weak and peculiar mode).

*Acknowledgments.* This research is supported by NSF Grant ATM-0647995. KK thanks Dr. Shang-Ping Xie for his suggestions. The authors acknowledge the

support from IPRC, which is in part sponsored by JAMSTEC and NASA. We also thank Ms. Di Henderson for her editorial work and two anonymous reviewers for their insightful and valuable comments. Interpolated OLR data and NCEP Reanalysis 2 data were provided by the NOAA/OAR/ESRL PSD, Boulder, Colorado, from their Web site at http://www.cdc.noaa.gov/. TRMM 3B42 data used in this study and the algorithm were acquired as part of the Tropical Rainfall Measuring Mission (TRMM) science team. The data were processed by the TRMM Science Data and Information System (TSDIS) and the TRMM Office; they are archived and distributed by the Goddard Distributed Active Archive Center. TRMM is an international project jointly sponsored by the Japan National Space Development Agency (NASDA) and the U.S. National Aeronautics and Space Administration (NASA) Office of Earth Sciences.

## REFERENCES

Chan, J. C. L., W. X. Wi, and J. J. Xu, 2002: Mechanisms responsible for the maintenance of the 1998 South China Sea summer monsoon. *J. Meteor. Soc. Japan,* **80,** 1103–1113.

Chatterjee, P., and B. N. Goswami, 2004: Structure, genesis and scale selection of the tropical quasi-biweekly mode. *Quart. J. Roy. Meteor. Soc.,* **130,** 1171–1194.

Chen, T.-C., and J.-M. Chen, 1993: The 10–20-day mode of the 1979 Indian monsoon: Its relation with the time variation of monsoon rainfall. *Mon. Wea. Rev.,* **121,** 2465–2482.

——, and ——, 1995: An observational study of the South China Sea monsoon during the 1979 summer: Onset and life cycle. *Mon. Wea. Rev.,* **123,** 2295–2318.

——, M. C. Yen, and S. P. Weng, 2000: Interaction between the summer monsoons in East Asia and the South China Sea: Intraseasonal monsoon modes. *J. Atmos. Sci.,* **57,** 1373–1392.

Chen, W. Y., 1982: Fluctuations in Northern Hemisphere 700 mb height field associated with the Southern Oscillation. *Mon. Wea. Rev.,* **110,** 808–823.

Drbohlav, H.-K. L., and B. Wang, 2005: Mechanism of the northward-propagating intraseasonal oscillation: Insights from a zonally symmetric model. *J. Climate,* **18,** 952–972.

Duchon, C. E., 1979: Lanczos filtering in one and two dimensions. *J. Appl. Meteor.,* **18,** 1016–1022.

Emery, W. J., and R. E. Thomson, 1997: *Data Analysis Methods in Physical Oceanography*. Elsevier, 638 pp.

Frank, W. M., and P. E. Roundy, 2006: The role of tropical waves in tropical cyclogenesis. *Mon. Wea. Rev.,* **134,** 2397–2417.

Gilman, D. L., F. J. Fuglister, and J. M. Mitchell Jr., 1963: On the power spectrum of red noise. *J. Atmos. Sci.,* **20,** 182–184.

Goswami, B. N., R. S. Ajayamohan, P. K. Xavier, and D. Sengupta, 2003: Clustering of synoptic activity by Indian summer monsoon intraseasonal oscillations. *Geophys. Res. Lett.,* **30,** 1431, doi:10.1029/2002GL016734.

Hoskins, B. J., and T. Ambrizzi, 1993: Rossby wave propagation on a realistic longitudinally varying flow. *J. Atmos. Sci.,* **50,** 1661–1671.

Huffman, G. J., and Coauthors, 2007: The TRMM Multisatellite Precipitation Analysis (TMPA): Quasi-global multiyear, combined-sensor precipitation estimates at fine scales. *J. Hydrometeor.,* **8,** 38–55.

Jiang, X., T. Li, and B. Wang, 2004: Structures and mechanisms of the northward propagating boreal summer intraseasonal oscillation. *J. Climate,* **17,** 1022–1039.

Kanamitsu, M., W. Ebisuzaki, J. Woollen, S. K. Yang, J. J. Hnilo, M. Fiorino, and G. L. Potter, 2002: NCEP–DOE AMIP-II reanalysis (R-2). *Bull. Amer. Meteor. Soc.,* **83,** 1631–1643.

Kiladis, G. N., and K. M. Weickmann, 1992: Extratropical forcing of tropical Pacific convection during northern winter. *Mon. Wea. Rev.,* **120,** 1924–1938.

——, and M. Wheeler, 1995: Horizontal and vertical structure of observed tropospheric equatorial Rossby waves. *J. Geophys. Res.,* **100,** 22 981–22 997.

——, and K. M. Weickmann, 1997: Horizontal structure and seasonality of large-scale circulations associated with submonthly tropical convection. *Mon. Wea. Rev.,* **125,** 1997–2013.

Krishnamurti, T. N., and H. Bhalme, 1976: Oscillations of a monsoon system. Part I: Observational aspects. *J. Atmos. Sci.,* **33,** 1937–1954.

——, and P. Ardanuy, 1980: 10- to 20-day westward propagating mode and ''Breaks in the Monsoons.'' *Tellus,* **32,** 15–26.

Lau, K.-H., and N.-C. Lau, 1990: Observed structure and propagation characteristics of tropical summertime synoptic scale disturbances. *Mon. Wea. Rev.,* **118,** 1888–1913.

Liebmann, B., and C. A. Smith, 1996: Description of a complete (interpolated) outgoing longwave radiation dataset. *Bull. Amer. Meteor. Soc.,* **77,** 1275–1277.

Madden, R. A., and P. R. Julian, 1971: Detection of a 40–50 day oscillation in the zonal wind in the tropical Pacific. *J. Atmos. Sci.,* **28,** 702–708.

——, and ——, 1972: Description of global-scale circulation cells in tropics with a 40–50 day period. *J. Atmos. Sci.,* **29,** 1109–1123.

——, and ——, 1994: Observations of the 40–50-day tropical oscillation: A review. *Mon. Wea. Rev.,* **122,** 814–837.

Mao, J. Y., and J. C. L. Chan, 2005: Intraseasonal variability of the South China Sea summer monsoon. *J. Climate,* **18,** 2388–2402.

Matsuno, T., 1966: Quasi-geostrophic motions in the equatorial area. *J. Meteor. Soc. Japan,* **44,** 25–43.

Murakami, M., 1975: Cloudiness fluctuations during summer monsoon. *J. Meteor. Soc. Japan,* **54,** 175–181.

——, and M. Frydrych, 1974: On the preferred period of upper wind fluctuations during the summer monsoon. *J. Atmos. Sci.,* **31,** 1549–1555.

Numaguti, A., 1995: Characteristics of 4–20-day-period disturbances observed in the equatorial Pacific during the TOGA COARE IOP. *J. Meteor. Soc. Japan,* **73,** 353–377.

Sardeshmukh, P. D., and B. J. Hoskins, 1984: Spatial smoothing on the sphere. *Mon. Wea. Rev.,* **112,** 2524–2529.

Tomas, R. A., and P. J. Webster, 1994: Horizontal and vertical structure of cross-equatorial wave propagation. *J. Atmos. Sci.,* **51,** 1417–1430.

von Storch, H., and F. W. Zwiers, 1999: *Statistical Analysis in Climate Research*. Cambridge University Press, 484 pp.

Waliser, D., 2006: Intraseasonal variations. *The Asian Monsoon,* B. Wang, Ed., Springer, 787 pp.

Wallace, J. M., and D. S. Gutzler, 1981: Teleconnections in the geopotential height field during the Northern Hemisphere winter. *Mon. Wea. Rev.,* **109,** 784–812.

Wang, B., and H. Rui, 1990: Synoptic climatology of transient tropical intraseasonal convection anomalies: 1975-1985. *Meteor. Atmos. Phys.,* **44,** 43–61.

——, and X. Xie, 1996: Low-frequency equatorial waves in vertically sheared zonal flow. Part I: Stable waves. *J. Atmos. Sci.,* **53,** 449–467.

Weare, B. C., and J. S. Nasstrom, 1982: Examples of extended empirical orthogonal function analyses. *Mon. Wea. Rev.,* **110,** 481–485.

Webster, P. J., and J. R. Holton, 1982: Cross-equatorial response to middle-latitude forcing in a zonally varying basic state. *J. Atmos. Sci.,* **39,** 722–733.

Wu, M.-L. C., S. D. Schubert, M. J. Suarez, and N. E. Huang, 2009: An analysis of moisture fluxes into the Gulf of California. *J. Climate,* in press.

Xie, X. S., and B. Wang, 1996: Low-frequency equatorial waves in vertically sheared zonal flow. Part II: Unstable waves. *J. Atmos. Sci.,* **53,** 3589–3605.

Yang, J., B. Wang, and B. Wang, 2008: Anticorrelated intensity change of the quasi-biweekly and 30–50-day oscillations over the South China Sea. *Geophys. Res. Lett.,* **35,** L16702, doi:10.1029/2008GL034449.

Yasunari, T., 1981: Structure of an Indian summer monsoon system with around 40-day period. *J. Meteor. Soc. Japan,* **59,** 336–354.

Zangvil, A., 1975: Upper tropospheric waves in the tropics and their association with clouds in the wavenumber-frequency domain. Ph.D. thesis, University of California, Los Angeles, 131 pp.

Zhang, C. D., 2005: Madden-Julian oscillation. *Rev. Geophys.,* **43,** RG2003, doi:10.1029/2004RG000158.

Zhou, S. T., and A. J. Miller, 2005: The interaction of the Madden–Julian oscillation and the Arctic Oscillation. *J. Climate,* **18,** 143–159.